EJN European Journal of Neuroscience

FENS Federation of European Neuroscience Societies

European Journal of Neuroscience, Vol. 40, pp. 3055–3066, 2014 doi:10.1111/ejn.12672

NEUROSYSTEMS

The role of the area postrema in the anorectic effects of amylin and salmon calcitonin: behavioral and neuronal phenotyping

Fiona E. Braegger,[1] Lori Asarian,[1,2] Kirsten Dahl,[3] Thomas A. Lutz[1,2,4] and Christina N. Boyle[1]
[1]Institute of Veterinary Physiology, University of Zurich, Zurich 8057, Switzerland
[2]Zurich Center of Integrative Human Physiology, Zurich, Switzerland
[3]NovoNordisk A/S, Maaloev, Denmark
[4]Institute of Laboratory Animal Science, University of Zurich, Zurich, Switzerland

Keywords: AP lesion, meal pattern analysis, noradrenaline, rat, VGLUT2

Abstract

Amylin reduces meal size by activating noradrenergic neurons in the area postrema (AP). Neurons in the AP also mediate the eating-inhibitory effects of salmon calcitonin (sCT), a potent amylin agonist, but the phenotypes of the neurons mediating its effect are unknown. Here we investigated whether sCT activates similar neuronal populations to amylin, and if its anorectic properties also depend on AP function. Male rats underwent AP lesion (APX) or sham surgery. Meal patterns were analysed under *ad libitum* and post-deprivation conditions. The importance of the AP in mediating the anorectic action of sCT was examined in feeding experiments of dose–response effects of sCT in APX vs. sham rats. The effect of sCT to induce Fos expression was compared between surgery groups, and relative to amylin. The phenotype of Fos-expressing neurons in the brainstem was examined by testing for the co-expression of dopamine beta hydroxylase (DBH) or tryptophan hydroxylase (TPH). By measuring the apposition of vesicular glutamate transporter-2 (VGLUT2)-positive boutons, potential glutamatergic input to amylin- and sCT-activated AP neurons was compared. Similar to amylin, an intact AP was necessary for sCT to reduce eating. Further, co-expression between Fos activation and DBH after amylin or sCT did not differ markedly, while co-localization of Fos and TPH was minor. Approximately 95% of neurons expressing Fos and DBH after amylin or sCT treatment were closely apposed to VGLUT2-positive boutons. Our study suggests that the hindbrain pathways engaged by amylin and sCT share many similarities, including the mediation by AP neurons.

Introduction

Amylin and calcitonin are structurally and functionally related peptides of the calcitonin-like gene peptide superfamily (Wimalawansa, 1997). Amylin and calcitonin share a common core receptor, the calcitonin receptor (CTR), which is transformed into a specific amylin receptor by receptor activity-modifying proteins (RAMPs; Sexton *et al.*, 1994; Christopoulos *et al.*, 1999; Muff *et al.*, 1999), specifically RAMP1 and RAMP3. Amylin is co-secreted with insulin from pancreatic β-cells (Butler *et al.*, 1990; Ogawa *et al.*, 1990), and one physiological response that amylin and calcitonin share is the inhibition of eating (Lutz *et al.*, 2000). While the anorectic action of mammalian calcitonin is relatively weak, fish-derived calcitonin, like salmon calcitonin (sCT), has often been used in pharmacological studies aimed at identifying the mechanism of action of amylin (Lutz *et al.*, 2000). In contrast to amylin, sCT displays stronger, irreversible receptor binding, which translates into a more potent, longer-lasting eating-inhibitory response (Riediger *et al.*, 1999; Lutz *et al.*, 2000; Reidelberger *et al.*, 2002).

Strong evidence suggests that the area postrema (AP) is an important brain site mediating amylin's anorectic effect (Lutz, 2012). Lesions of the AP and its amylin receptor population abolish peripheral amylin's eating-inhibitory effects (Lutz *et al.*, 1998, 2001; Mack *et al.*, 2010). Administration of exogenous peripheral amylin induces a strong Fos response in the AP and in several downstream nuclei, including the nucleus of the solitary tract (NTS; Rowland *et al.*, 1997; Rowland & Richmond, 1999; Barth *et al.*, 2004; Riediger *et al.*, 2004). The neurochemical phenotypes of the neurons mediating the inhibitory effects of amylin and sCT on eating are only partially identified. Approximately 50% of amylin-activated cells expressing Fos protein within the AP were also positive for the specific noradrenergic marker, dopamine beta hydroxylase (DBH; Potes *et al.*, 2010b). These DBH-positive neurons seem to be functionally relevant, because ablating them with saporin toxin reduced the anorectic action of amylin (Potes *et al.*, 2010b). It is unknown which neuronal populations are specifically activated by sCT, and whether sCT also activates the same noradrenergic population as amylin.

Correspondence: Dr C. N. Boyle, as above.
E-mail: boyle@vetphys.uzh.ch

T.A.L. and C.N.B. contributed equally to this work.

Received 10 January 2014, revised 11 June 2014, accepted 16 June 2014

More generally, ablating the AP not only prevents the anorectic effect of amylin, but also alters physiological feedback mechanisms that lead to a disruption in meal patterns (Ritter & Edwards, 1984; Stricker *et al.*, 1997). Hence, to further probe the role of the AP in the control of food intake, we first aimed to analyse meal patterns in our rat model of AP lesions (APX), compared with sham-lesioned rats. Our second goal was to determine whether equipotent doses of amylin and sCT activate phenotypically similar neuronal populations in the AP. To this end, we assessed whether the amylin- or sCT-induced Fos expression co-localizes with markers for catecholaminergic and serotoninergic neurons. Finally, because glutamatergic transmission may underlie several effects mediated by noradrenergic AP neurons (Stornetta *et al.*, 2002), and because this may be relevant for amylin-induced activation of the AP (Fukuda *et al.*, 2013), we evaluated the apposition of vesicular glutamate transporter-2 (VGLUT2)-positive boutons to neurons co-expressing Fos and DBH in the AP after amylin or sCT.

Materials and methods

Animals

Male Wistar rats (200–250 g; Charles River, Sulzfeld, Germany) were maintained at a constant ambient temperature (21 ± 1 °C) under an artificial 12 h light/dark cycle with standard chow diet (no. 3430; Provimi Kliba, Gossau, Switzerland) and water available *ad libitum*, unless otherwise noted. All experiments were performed with the approval of the Veterinary Office of the Canton Zurich, Switzerland, and in accordance with the EU Directive 2010/63/EU on the protection of animals used for scientific purposes.

Drugs

Amylin and sCT (Bachem AG, Bubendorf, Switzerland; catalog numbers: amylin H-9475.1000; sCT H-2260.0001) were reconstituted with sterile 0.9% saline and diluted with saline to final doses of 1, 5 or 10 μg/kg, with an injection volume of 1 mL/kg.

Surgery

Rats were anesthetized intraperitoneally (i.p.) using a mixture of ketamine (50 mg/kg; Narketan, Vétoquinol AG, Ittingen, Switzerland), xylazine (2.5 mg/kg, Xylazin; Streuli Pharma AG, Uznach, Switzerland) and acepromazine (0.75 mg/kg, Prequillan; Arovet AG, Dietikon, Switzerland). The head of the rat was flexed ventrally at an approximate 110 ° angle in a stereotaxic frame. Skin and three layers of neck musculature were cut and retracted for visualization of the foramen magnum. Under visual control with a surgical microscope, the cranial dura mater was penetrated with an angled cannula tip and the cerebrospinal fluid was blotted. AP lesions were performed by aspirating the AP with a blunted cannula tip fixed to a flexible tube attached to a vacuum pump (Lutz *et al.*, 1998; Jordi *et al.*, 2013). In sham-lesioned rats, the AP was exposed but not touched. Musculature and skin were sutured respecting the individual muscle layers. Rats received subcutaneous injections of 5 mL sterile saline, antibiotics (7.5 mg/kg enrofloxacin, Baytril 2.5%; Provet AG, Lyssach, Switzerland) and an analgesic (1 mg/kg flunixin, Fluniximin; Graeub AG, Bern, Switzerland) daily for at least 3 days post-surgery, and were given 1–2 weeks to recover from surgery. At the end of the experiments AP lesions were confirmed histologically (Lutz *et al.*, 1998, 2001; Riediger *et al.*, 2004), in parallel with the immunohistochemical quantification.

Experiment 1: meal pattern analysis in untreated AP-lesioned and sham-lesioned rats

Meal patterns in sham- and AP-lesioned groups (n = 16 and 13, respectively) were analysed using the BioDAQ Food Intake Monitor (Research Diets, New Brunswick, NJ, USA). The technical specifications of the monitoring system have been described previously (Boyle *et al.*, 2011). Rats were habituated to a 12-h fast twice per week followed by 3 days of adaptation to the BioDAQ cages (type 2000P; Tecniplast, Germany). Meal pattern data were collected and analysed under two conditions. First, eating was recorded for 24 h in *ad libitum*-fed rats. Second, 24-h food intake data were collected after a 12-h fast during the light phase. Meal pattern data collected from each rat were segmented into meals by clustering independent feeding bouts. The criteria defining a meal were a minimum inter-meal interval of 15 min and a minimum meal size of 0.23 g. Data were analysed using the BioDAQ Monitoring software.

Experiment 2: behavioral experiments: dose–response study and identification of equipotent eating-inhibitory doses of amylin and sCT

Sham-lesioned and APX rats were individually housed in hanging wire mesh cages (Indulab AG, Gams, Switzerland; stainless steel, 47 × 33 × 20 cm) fitted with external food hoppers. Twice per week, rats were fasted for 12 h during the light phase. Shortly before dark-onset, rats were injected i.p. with vehicle (0.9% saline), amylin or sCT; at dark-onset, food was given back. Food intake was measured manually using a digital scale after 1, 2, 4 and 24 h. Tests were repeated in a randomized, crossover manner, so that each animal within the surgery group was examined under all treatment conditions. The dose–response relationships for amylin and sCT were assessed using three increasing doses (1, 5, 10 μg/kg). Based on these findings, equipotent doses of amylin (10 μg/kg) and sCT (5 μg/kg) were tested again in a different group of rats, in a second behavioral experiment.

Experiments 3–5: phenotypic characterization of amylin- and sCT-activated neurons

Rats were fasted for 12 h during the light phase before receiving injections of vehicle, amylin (10 μg/kg) or sCT (5 μg/kg) at dark-onset. Food was withheld and, 90 min later, rats were deeply anesthetized with pentobarbital (100 mg/kg, i.p.; Cantonal Pharmacy of Zurich, Switzerland), transcardially perfused with 4% paraformaldehyde in 0.1 M phosphate buffer (PB), and brains collected.

Perfused brains were kept in 4% paraformaldehyde for 48 h, followed by cryoprotection in 0.1 M PB (pH 7.2) containing 20% sucrose for 24 h. Brains were then frozen with hexane (Sigma Aldrich) on dry ice. Six series of 30-μm-thick frontal sections (from bregma −6.36 mm to −14.40 mm) were cut on a cryostat (Leica microsystems, Wetzlar, Germany). The sections were kept in a cryoprotecting medium (50% 0.1 M PB, 30% ethylene glycol, 20% glycerol) at −20 °C until processing for immunohistochemistry. One series of sections from each brain was processed for the detection of Fos and DBH, one series for the detection of Fos and tryptophan hydroxylase (TPH), and one series was processed for the detection of Fos, DBH and VGLUT2.

Experiment 3: double-immunostaining for Fos and DBH

All rinses were conducted in 0.1 M PB for 10 min. At least four rinses were implemented between every incubation step. Free-floating sections were incubated for 1 h at room temperature in a blocking

solution of 0.1 M PB containing 1% normal donkey or normal goat serum (NDS or NGS) and 0.3% Triton-X (Triton X-100; Sigma Aldrich, Germany). The primary and secondary antibodies were diluted in 0.1 M PB containing 1% NDS or NGS and 0.3% Triton-X at concentrations described in Table 1. Sections were incubated in the two primary antibody solutions for subsequent overnights (beginning with the Fos antibody) at room temperature, followed by 1-h incubation in fluorochrome-conjugated secondary antibody solutions at room temperature. Stained sections were mounted on gelatinized slides and coverslipped with Citifluor (AF-100; Citifluor, London, UK).

Experiment 4: double-immunostaining for Fos and TPH

All rinses were conducted in 0.1 M PB for 10 min. At least four rinses were implemented between every incubation step. Free-floating sections were blocked for 1 h at room temperature in 0.1 M PB containing 1% NDS and 0.3% Triton-X (Sigma Aldrich). Sections were incubated overnight at room temperature in the anti-Fos primary antibody diluted in 0.1 M PB, 1% NDS and 0.3% Triton-X. Thereafter, sections were incubated in the corresponding secondary antibody (Table 1) diluted in 0.1 M PB, 1% NDS and 0.3% Triton-X for 1 h at room temperature. After the incubation with the secondary antibody, the tissue was incubated for 1 h at room temperature in an Avidin/Biotinylated enzyme Complex (ABC) solution. For visualization of Fos-positive cells, sections were incubated in enhanced 3,3′-diaminobenzidine-tetrahydrochloride (DAB) chromogen solution (0.05% DAB, 0.04% nickel, 0.08% cobalt and 0.3% H_2O_2 in phosphate-buffered saline) for approximately 2–5 min. Next, the tissue was incubated in the anti-TPH primary antibody overnight at room temperature and the following day, in the corresponding secondary antibody for 1 h. To visualize TPH-positive cells, a peroxidase substrate system (ImmPACT NovaRED; Vector Laboratories, Burlingame, CA, USA) was used. The sections were incubated in the peroxidase substrate for 2–5 min, and then rinsed in distilled water to stop the staining process and wash off the remaining reagents. All concentrations of antibody and chromogen solutions are shown in Table 1. Tissue was mounted on gelatinized slides and left to air dry for up to 1 h. Slides were then dehydrated in an ascending series of clean alcohols, defatted in xylol and coverslipped with DPX medium (Fisher Scientific, Reinach, Switzerland).

Quantification and analysis of double-immunostaining

Photomicrographs of all sections containing AP, medial subnucleus of the NTS (mNTS), dorsal and central raphe nuclei (DR, CR) were taken at 20 × magnification and a numeric aperture of 0.5, using a light microscope (Zeiss Imager Z2) fitted with a black and white camera (Zeiss Axiocam HRm) or a color camera (Zeiss Axiocam). Fos-positive cells were counted using ImageJ software (National Institutes of Health, Bethesda, MD, USA). All other quantifications were done manually in a blinded manner, counting by eye using the digital images. Sections within the following bregma coordinates were quantified: −13.56 to −14.40 mm for the AP, −11.76 to –14.40 mm for the NTSm, −6.36 to −9.36 mm for the DR and CR. For each animal, the counts from all sections (corresponding to a particular brain area) were averaged. Final results are reported as group means ± SEM. For the remainder of the manuscript this method of imaging and quantification will be referred to as light microscopy.

Experiment 5: triple-immunostaining for Fos, DBH and VGLUT-2

Rinses were conducted as above. All incubation and blocking steps were conducted at room temperature. Free-floating sections were first blocked in sequential blocking solutions consisting of 0.1 M PB and Avidin (1 : 10) or Biotin (1 : 10), for 15 min each, followed by blocking in 0.3% Triton-X and 1% NDS in 0.1 M PB for 1 h. Sections were then incubated overnight in a 0.1 M PB solution containing 0.3% Triton-X, 1% NDS and all three primary antibodies (anti-Fos, -DBH and -VGLUT2). On the following day, sections were incubated for 1 h in a solution of 0.1 M PB containing 0.3% Triton-X, 1% NDS and all three fluorochrome-conjugated secondary antibodies (Table 1). Stained sections were then mounted on gelatinized slides and coverslipped with Citifluor.

Quantification and analysis of triple-immunostaining

In order to have 3D visualization of the VGLUT2-positive boutons and their proximity to neurons double-labeled for Fos and DBH, confocal image acquisition was required. Stereological methods were then applied to these 3D images to quantify the presence of Fos, DBH and VGLUT2 immunostaining in the entire AP. All brain sections containing the AP were scanned with a CLSM Leica SP5 Mid UV-VIS confocal microscope equipped with an *x–y–z* motorized stage and lasers appropriate for detecting Cy3, Alexa 488 and Alexa 647 fluorescence. Scans were taken in the tile mode using a 63 × magnification and a numeric aperture (oil immersion) of 1.4. The extent of the AP was marked manually (*x*/*y* positions) and the software (LASF, advanced fluorescence lite, 2.6.0; Leica microsystems, Wetzlar, Germany) adjusted the total number of tiles to be scanned.

TABLE 1. Immunohistochemical reagents

Reagents	Antigen/conjugate	Host	Type	Source	Catalog no.	Dilution
Primary	Fos	Rb	Polyclonal	Calbiochem	PC38	1 : 10 000
Secondary	Anti-rabbit IgG	Dk	Cy3-labeled	Jackson	711-165-152	1 : 400
Secondary	Anti-rabbit IgG	Dk	Biotinylated	Jackson	711-065-152	1 : 400
Primary	DBH	Ms	Monoclonal	Millipore	MAB308	1 : 1000
Secondary	Anti-mouse IgG	Dk	Alexa488-labeled	Jackson	715-545-150	1 : 400
Primary	TPH	Sh	Polyclonal	Millipore	AB1541	1 : 5000
Secondary	Anti-sheep IgG	Dk	Biotinylated	Jackson	713-065-003	1 : 400
Primary	VGLUT2	Gp	Polyclonal	Millipore	AB5907	1 : 2000
Secondary	Anti-guinea pig	Dk	Alexa647-labeled	Jackson	706-605-148	1 : 400
Immune-peroxidase	ABC system		Vectastain Elite ABC kit	Vector	PK-6100	1 : 400
Chromagen	DAB			Sigma	D5637	1 : 20
Peroxidase substrate	ImmPact NovaRed			Vector	SK4805	

Rb, rabbit; Dk, donkey; Ms, mouse; Sh, sheep; Gp, guinea pig; DAB, 3,3′-diaminobenzidine-tetrahydrochloride; DBH, dopamine beta hydroxylase; TPH, tryptophan hydroxylase; VGLUT2, vesicular glutamate transporter-2.

At three randomly chosen *x*/*y* coordinates in each section, the thickness of the section was measured manually and then used to define the *z*-height of all tiles to be scanned at *z*-increments of 0.5 μm. An overlap of 15% was used for the subsequent stitching of the tiles to generate a complete 3D image of the AP section.

Using the Optical Fractionator (Stereo Investigator 10; MBF Bioscience, Williston, VT, USA; as described previously by West *et al.*, 1991), Fos-positive, DBH-positive, Fos- and DBH-double-positive cells and VGLUT2-positive boutons were counted using a counting frame size of 80 × 80 μm, a dissector height of 10 μm and a top guard zone of 2 μm. Only VGLUT2-positive boutons that were abutting a neuron's soma were considered. All boutons in apposition to Fos- and DBH-double-positive cells selected by the optical dissector probe were counted. Unbiased estimates of the total number of neurons of interest per AP were acquired by multiplying the counts with the inverse of the sampling fractions for sections, area and section thickness. This method of confocal stereological quantification will be referred to as confocal microscopy for the remainder of the manuscript.

Statistics

Statistical analysis was done using Prism (Graph Pad Software, La Jolla, CA, USA). One-way ANOVA and Student's *t*-tests were used as described below. One-way ANOVA analyses were followed by Bonferroni *post hoc* tests, when appropriate. A *P*-value of < 0.05 was considered statistically significant for all experiments.

- Experiment 1: *t*-tests; sham vs. APX within *ad libitum* or post-deprivation conditions, $n = 13–17$ per surgery group.
- Experiment 2: one-way ANOVA; treatment as main factor, within surgery (APX or sham) condition, per time point, $n = 11–13$ per surgery group.
- Experiment 3: one-way ANOVA; treatment as main factor, within surgery (APX or sham) condition, $n = 13–17$ per surgery group.
- Experiment 4: one-way ANOVA; treatment as main factor, within surgery (APX or sham) condition, $n = 13–17$ per surgery group.
- Experiment 5: *t*-tests; amylin 10 μg/kg vs. sCT 5 μg/kg within sham-lesioned rats, $n = 5–6$ per treatment group.
- Experiment 6: *t*-tests; comparison of quantitative analysis using confocal microscopy vs. light microscopy within treatment condition (amylin 10 μg/kg or sCT 5 μg/kg), $n = 5–6$ per treatment group.

Results

Experiment 1: meal pattern analysis of sham and APX rats

APX rats exhibited altered meal patterns indicative of a change in feedback inhibition of ingestive behavior. Under *ad libitum* conditions, the size of the first meal was significantly larger in APX than sham rats ($t_{26} = 5.425$, $P < 0.001$), but APX rats took longer after dark-onset to initiate the first meal ($t_{26} = 3.028$, $P = 0.006$). Average meal size ($t_{26} = 3.870$, $P < 0.001$) as well as average meal duration ($t_{26} = 2.192$, $P = 0.038$) were significantly increased in APX compared with sham rats. Although sham rats ate more meals per day than APX rats ($t_{26} = 3.564$, $P = 0.001$), the inter-meal interval was not significantly different. Total 24-h food intake did not differ between sham and APX rats (Table 2).

In the post-deprivation condition following a 12-h light-phase fast, food intake of APX rats in the following 24 h was significantly reduced compared with sham ($t_{26} = 3.128$, $P = 0.004$). Similar to *ad libitum* conditions, APX rats consumed significantly fewer meals ($t_{26} = 5.728$, $P < 0.0001$) and their latency to feed after dark-onset was longer ($t_{26} = 5.650$, $P < 0.0001$). Average meal size, meal duration, size of first meal and the inter-meal interval did not differ significantly between the two surgery groups in this state, which was largely due to a deprivation-induced increase in meal size in the sham group that was not observed in the APX group.

Experiment 2.1: dose–response curve

As previously reported (Lutz *et al.*, 2000), amylin and sCT dose-dependently decreased eating in sham rats (Fig. 1A and C). Eating was significantly decreased by 5 and 10 μg/kg amylin at the 1-h time point ($F_{3,12} = 7.034$, $P < 0.01$), and by 10 μg/kg amylin at the 2-h time point ($F_{3,12} = 5.941$, $P < 0.01$). A dose of 1 μg/kg amylin had no effect on eating, and none of the doses decreased eating at the 4-h time point ($F_{3,12} = 1.415$, $P > 0.05$). Amylin did not decrease eating in APX rats at any dose or time point ($F_{3,12} = 0.4145$, 0.6527 and 0.9649, for 1-, 2- and 4-h time points, respectively, $P > 0.05$ for all; Fig. 1B).

Compared with saline and 1 μg/kg sCT, 5 and 10 μg/kg sCT reduced food intake at all times ($F_{3,14} = 38.07$, 40.16, 67.14 and 401.6 for 1-, 2-, 4- and 24-h time points, respectively, $P < 0.001$) in sham rats. Doses of 5 and 10 μg/kg sCT were not significantly different from each other. A dose of 1 μg/kg sCT decreased eating only at 4 and 24 h post-injection ($F_{3,14} = 67.14$ and 401.6, for 4- and 24-h time points, respectively, $P < 0.001$). The AP lesion almost completely blocked the effect of sCT on eating. However, after receiving 5 μg/kg sCT, 4-h food intake in APX rats was significantly reduced, as shown by a one-way ANOVA and subsequent Bonferroni *post hoc* analysis (4-h; $F_{3,13} = 3.545$, $P < 0.05$; Fig. 1D).

Experiment 2.2: equipotent doses of amylin and sCT

Figure 2A shows the significant food intake reduction after amylin and sCT in sham rats; in the first hour after injection, 10 μg/kg amylin and 5 μg/kg sCT reduced food intake to a similar extent

TABLE 2. Mean ± SEM meal parameters measured in sham and APX rats under *ad libitum* conditions and following a 12-h light phase fast

	Ad libitum			Post-deprivation		
	Sham mean ± SEM	APX mean ± SEM	*P*-values	Sham mean ± SEM	APX mean ± SEM	*P*-values
Total food intake/24 h (g)	28.0 ± 0.7	28.1 ± 1.8	0.9438	31.4 ± 1	23.2 ± 2.7	0.0042
Total meal number/24 h	8.0 ± 0.4	5.9 ± 0.5	0.0014	7.7 ± 0.4	4.6 ± 0.3	< 0.0001
Average meal size (g)	3.6 ± 0.2	5.0 ± 0.3	0.0007	4.3 ± 0.3	5.4 ± 0.5	0.0537
Meal duration (min)	30.6 ± 2.9	41.5 ± 4.3	0.0375	37.2 ± 4.5	44.9 ± 4.2	0.2360
First meal size (g)	2.7 ± 0.2	5.4 ± 0.5	<0.001	5.5 ± 0.7	5.2 ± 0.5	0.7456
Inter-meal interval (min)	65.8 ± 5.3	60.9 ± 6.9	0.5785	75.1 ± 6.1	82.3 ± 20.8	0.7099
Latency to feed (min)	10.3 ± 3.9	47.7 ± 13.3	0.0055	1.2 ± 0.3	60.6 ± 12.2	< 0.0001

APX, area postrema lesion.

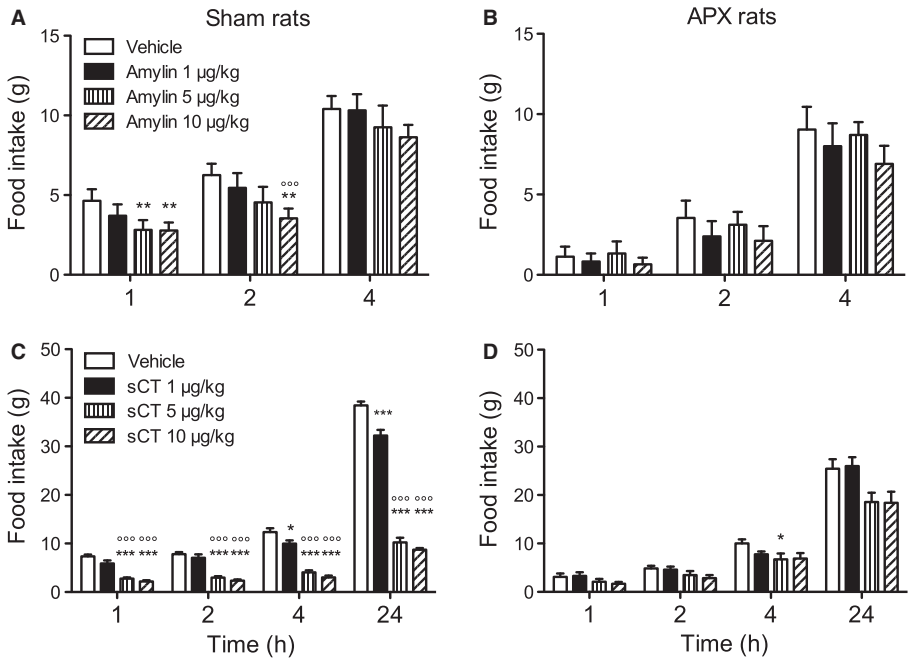

FIG. 1. Amylin and salmon calcitonin (sCT) lead to a dose-dependent reduction in cumulative food intake; the effect of sCT was more potent and longer lasting. Mean ± SEM cumulative food intake 1, 2, 4 and 24 h after injection of vehicle, amylin (1, 5 or 10 µg/kg; A, B) or sCT (1, 5 or 10 µg/kg; C, D) in sham-lesioned (A, C) and area postrema-lesioned (APX) rats (B, D). *Significantly different from vehicle $P \leq 0.05$, **$P \leq 0.01$, ***$P \leq 0.001$; °°°significantly different from 1 µg/kg $P \leq 0.001$.

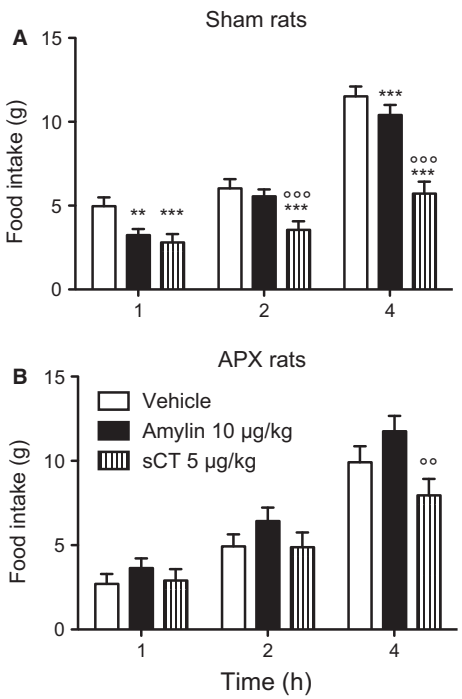

FIG. 2. Amylin (10 µg/kg) and salmon calcitonin (sCT; 5 µg/kg) reduced cumulative food intake similarly in sham rats in the first hour after injection compared with vehicle. Neither amylin nor sCT reduced eating in area postrema-lesioned (APX) rats compared with control. Mean ± SEM cumulative food intake 1, 2 and 4 h after injection of vehicle, amylin (10 µg/kg) or sCT (5 µg/kg) in sham-lesioned (A) and APX rats (B). **Significantly different from vehicle $P \leq 0.01$, ***$P \leq 0.001$; °°significantly different from amylin (10 µg/kg) $P \leq 0.01$, °°°$P \leq 0.001$.

($F_{2,16} = 13.17$, $P < 0.001$), and there was no significant difference in the eating-inhibitory effect of the two peptides at this time point. Two and 4 h after injection, only sCT but not amylin reduced eating. In the APX rats (Fig. 2B), neither peptide evoked a significant reduction of the cumulative food intake in the first 2 h. However, there was a significant difference 4 h after the injection between sCT and amylin, but not vehicle controls (one-way repeated-measures ANOVA and Bonferroni *post hoc* analysis; $F_{2,12} = 7.112$, $P < 0.01$).

Experiment 3: co-localization of Fos- and DBH-positive neurons in the AP and NTS

Amylin and sCT induced Fos in DBH-expressing neurons in the AP and NTS, as depicted in Fig. 3A–D. One-way ANOVA followed by a Bonferroni *post hoc* analysis revealed that 5 µg/kg of sCT produced significantly more Fos-positive cells ($F_{2,14} = 122.7$, $P < 0.05$) and neurons double-labeled for Fos and DBH than 10 µg/kg of amylin ($F_{2,14} = 71.7$, $P < 0.05$) in the AP (Fig. 4A). Relative co-activation was similar, with approximately 44% of the amylin-induced and 47% of the sCT-induced Fos-positive neurons being also positive for DBH; there was no difference between these percentages ($t_5 = 0.7585$, $P = 0.4823$). Further, there was no significant difference in number of DBH-positive cells across the treatment groups ($F_{2,14} = 1.431$, $P = 0.272$; Fig. 4A).

Compared with vehicle, both amylin and sCT treatment resulted in a significant increase in Fos in the NTS of sham rats ($F_{2,14} = 12.36$, $P < 0.001$; Fig. 4B). Amylin (10 µg/kg) led to a higher number of double-stained neurons ($F_{2,14} = 14.53$, $P < 0.05$) and a greater number of DBH-positive cells than sCT (5 µg/kg; $F_{2,14} = 12.45$, $P < 0.01$). Overall, the percentage of co-localization was much lower than in the AP. Neither amylin nor sCT induced Fos expression in the NTS of AP-lesioned rats (Fig. 4C). There was

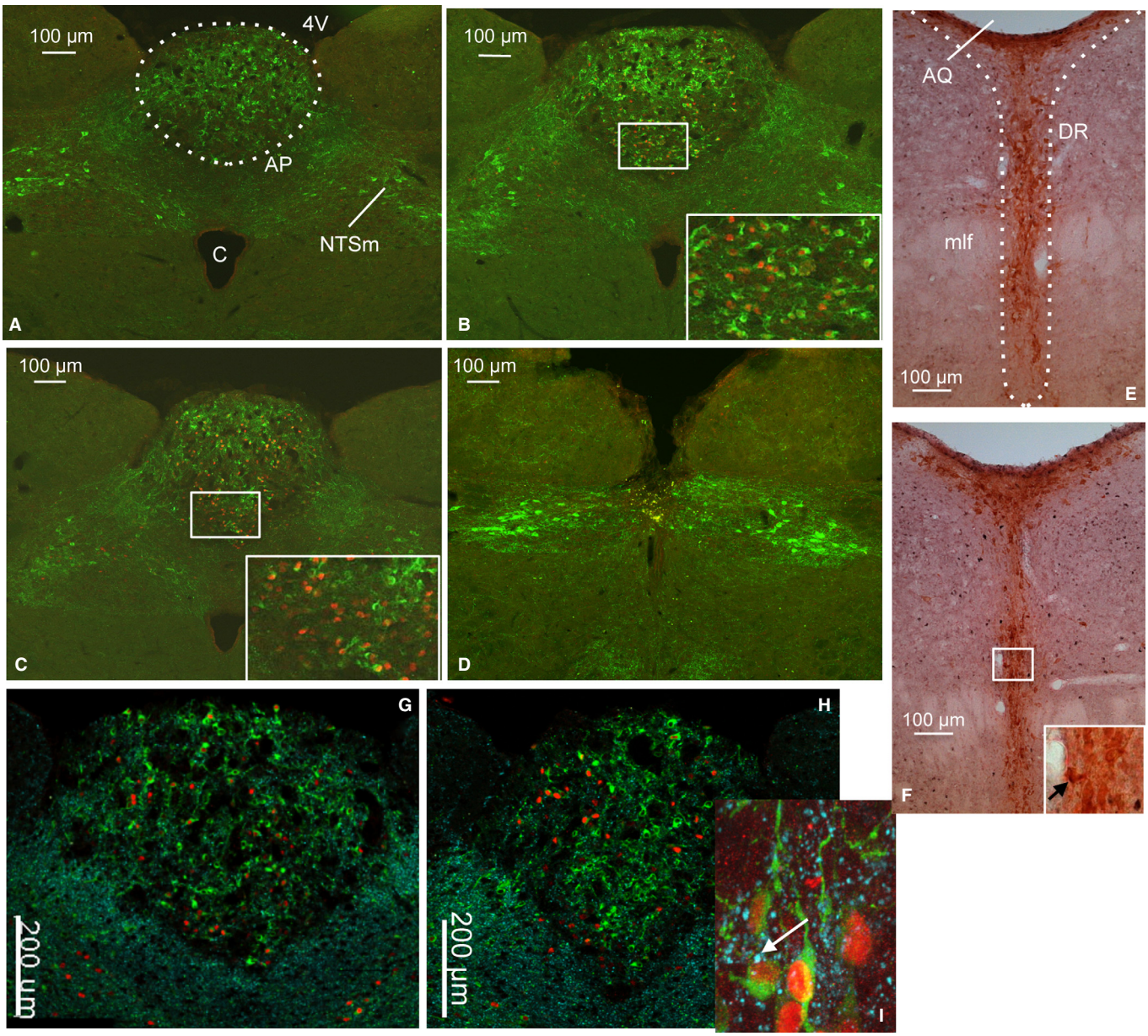

FIG. 3. Amylin and salmon calcitonin (sCT) induced Fos in dopamine beta hydroxylase (DBH)- but not tryptophan hydroxylase (TPH)-expressing neurons in brainstem nuclei. Representative images showing co-localization of Fos- (red nuclei) and DBH-expressing (green cell bodies) neurons in the area postrema (AP) and nucleus of the solitary tract (NTS) of sham rats after saline (A), amylin (10 µg/kg; B) or sCT (5 µg/kg; C) treatment, and in an AP-lesioned (APX) rat after amylin (10 µg/kg; D). Representative images showing minimal co-localization of Fos- (black nuclei) and TPH-expressing (dark orange cell bodies and processes) neurons in the dorsal raphe nucleus (DR) of sham (E) and APX (F) rats treated with 5 µg/kg sCT; the inset in (F) shows an example of one neuron co-expressing Fos and TPH (black arrow). Representative images showing the co-localization of Fos (red nuclei), DBH (green cell bodies) and vesicular glutamate transporter-2 (VGLUT2; cyan boutons) in the AP of sham rats treated with 10 µg/kg amylin (G) or 5 µg/kg sCT (H). The inset shows a high-magnification confocal scan of AP from sham rat treated with 5 µg/kg sCT showing an example of VGLUT2 bouton (white arrow) apposed to a neuron co-expressing Fos and DBH (I). AQ, cerebral aqueduct; C, central canal; mlf, medial longitudinal fascicle; NTSm, medial subnucleus of the nucleus of the solitary tract; 4V, fourth ventricle.

no significant difference in the number of DBH-positive cells between the treatment groups ($F_{2,10} = 3.357$, $P = 0.0766$).

Experiment 4: co-localization of Fos- and TPH-positive neurons in brainstem nuclei

Amylin (10 µg/kg) and sCT (5 µg/kg) significantly increased the number of Fos-positive cells in the AP compared with vehicle (one-way ANOVA and Bonferroni *post hoc* analysis; $F_{2,14} = 67.25$, $P < 0.0001$); however, no TPH-positive neurons were detected in either group (Fig. 5A). Amylin (10 µg/kg) and sCT (5 µg/kg) significantly increased the number of Fos-positive cells in the NTS of sham-lesioned rats ($F_{2,14} = 18.35$, $P = 0.0001$; Fig. 5B). Amylin and sCT treatment did not significantly alter the number of TPH-positive cells in the NTS of sham rats, and there was no appreciable overlap of Fos and TPH staining in any of the three groups. Following APX (Fig. 5C), the number of amylin- and sCT-induced Fos-positive cells in the NTS was indistinguishable from vehicle-treated rats.

One-way ANOVA analysis suggested that a constitutive amount of Fos, TPH and a low degree of co-localization (Table 3) of these two

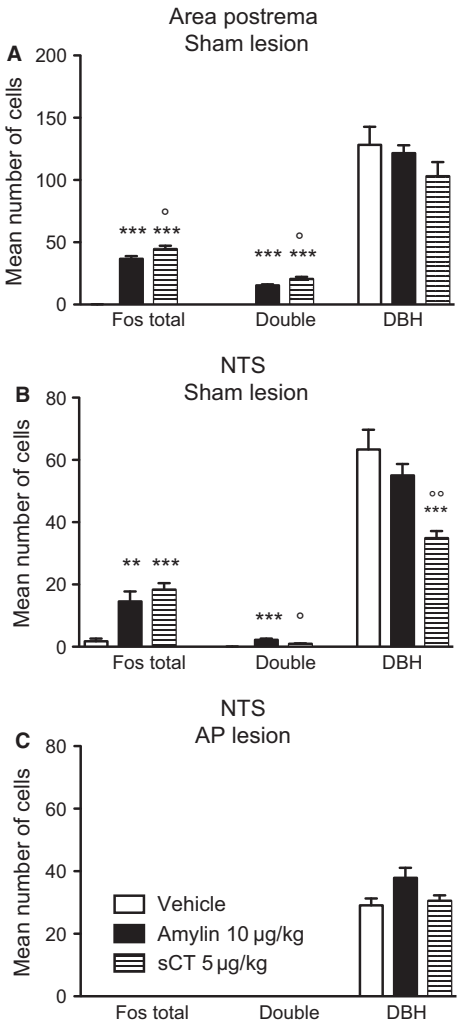

FIG. 4. Amylin and salmon calcitonin (sCT)-induced Fos co-localizes with dopamine beta hydroxylase (DBH)-positive neurons in the area postrema (AP) and nucleus of the solitary tract (NTS) of sham rats. Mean ± SEM number of Fos-positive, DBH-positive and double-labeled cells in the AP (A) and NTS (B) of sham rats, and the NTS of AP-lesioned (APX) rats (C) after treatment with vehicle, amylin (10 µg/kg) or sCT (5 µg/kg). **Significantly different from vehicle $P \leq 0.01$, ***$P \leq 0.001$; °significantly different from amylin (10 µg/kg) $P \leq 0.05$, °°$P \leq 0.01$.

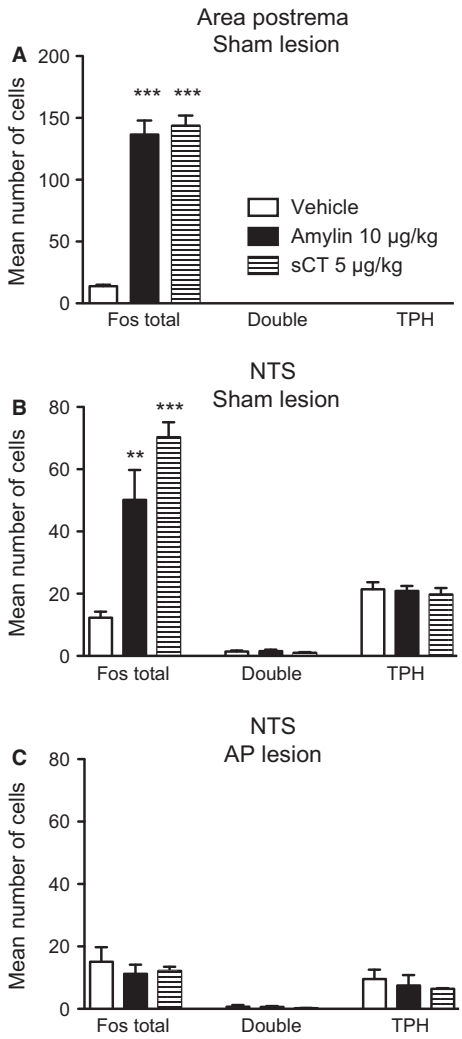

FIG. 5. Amylin and salmon calcitonin (sCT)-induced Fos does not co-localize with tryptophan hydroxylase (TPH)-positive neurons in the area postrema (AP) and nucleus of the solitary tract (NTS) of sham rats. Mean ± SEM number of Fos-positive, TPH-positive and double-labeled cells in the AP (A) and NTS (B) of sham rats, and the NTS of AP-lesioned (APX) rats (C) after treatment with vehicle, amylin (10 µg/kg) or sCT (5 µg/kg). **Significantly different from vehicle $P \leq 0.01$, ***$P \leq 0.001$.

markers seemed to be present in the DR and CR (Fig. 3E and F), independent of treatment and surgery (sham vs. APX).

Experiment 5: co-localization of Fos- and DBH-positive neurons apposed to VGLUT2-positive boutons in the AP

Confocal microscopy analysis revealed that rats treated with sCT exhibited a significantly greater number of Fos-positive cells in the AP compared with amylin-treated rats ($t_9 = 3.157$, $P = 0.0116$; Fig. 6A), this coincides with the results acquired with the standard light microscopy method. Confocal analysis also revealed that amylin and sCT did not alter the number of DBH-positive cells in the AP ($t_9 = 0.3311$, $P = 0.7482$; Fig. 6B). There was a significant difference in the number of double-labeled cells between amylin and sCT ($t_9 = 3.094$, $P = 0.0128$), as shown in Fig. 6C, but the percentage of co-localization did not differ between amylin and sCT. Furthermore, there was no significant difference in the total number of VGLUT2-positive boutons ($t_9 = 2.082$, $P = 0.067$; Fig. 6D) or the number of VGLUT2-positive boutons per double-labeled cell ($t_9 = 0.5655$, $P = 0.5855$; Fig. 6E) when comparing sCT- and amylin-treated groups. In amylin-treated sham rats, an average of 94.6% of all cells co-expressing Fos and DBH were apposed to VGLUT2-positive boutons, vs. a mean of 95.2% for sCT; these percentages did not differ significantly ($t_9 = 0.2411$, $P = 0.8149$). Representative confocal images are shown in Fig. 3G–I.

Based on the Gunderson–Jensen estimator (Gundersen *et al.*, 1999), using a smoothness constant of 1 for the AP, the ratio between mean CE^2 and the observed relative variance CV^2 was < 0.5 for all the markers estimated, demonstrating that the sampling procedure contributed only little to the observed group variances.

Experiment 6: comparison of the two methods of quantification

When comparing the results obtained with confocal microscopy with those obtained with light microscopy, we did not detect a significant difference in the percentage of Fos cells that were double-labeled for Fos and DBH following amylin ($t_5 = 0.1353$, $P = 0.8977$) or

TABLE 3. Mean ± SEM number of Fos-positive, TPH-positive and double-labeled cells in the DR and CR of sham and APX rats after treatment with vehicle, amylin (10 μg/kg) or sCT (5 μg/kg)

	Sham			APX		
	Vehicle mean ± SEM	Amylin 10 μg/kg mean ± SEM	sCT 5 μg/kg mean ± SEM	Vehicle mean ± SEM	Amylin 10 μg/kg mean ± SEM	sCT 5 μg/kg mean ± SEM
DR						
Fos-positive	9.6 ± 4.3	20.3 ± 5.2	7.2 ± 2.4	6.5 ± 2.5	19.6 ± 6.6	12.0 ± 7.4
Double-labeled (Fos + TPH)	2.4 ± 1.3	8.2 ± 3.0	1.8 ± 0.6	0.9 ± 0.5	4.9 ± 2.4	4.5 ± 3.1
TPH-positive	100.6 ± 5.7	117.7 ± 12.1	114.6 ± 22.7	116.4 ± 13.6	109.0 ± 13.2	101.9 ± 13.1
CR						
Fos-positive	4.4 ± 2.4	8.1 ± 3.0	3.5 ± 1.2	4.0 ± 1.8	10.7 ± 4.7	7.5 ± 3.0
Double-labeled (Fos + TPH)	1.1 ± 0.7	2.4 ± 0.8	1.6 ± 0.8	0.4 ± 0.1	2.5 ± 1.2	1.1 ± 0.6
TPH-positive	49.6 ± 7.5	57.1 ± 3.9	53.6 ± 5.7	49.6 ± 2.9	54.9 ± 1.8	49.7 ± 3.7

APX, area postrema lesion; CR, central raphe nucleus; DR, dorsal raphe nucleus; sCT, salmon calcitonin; TPH, tryptophan hydroxylase.

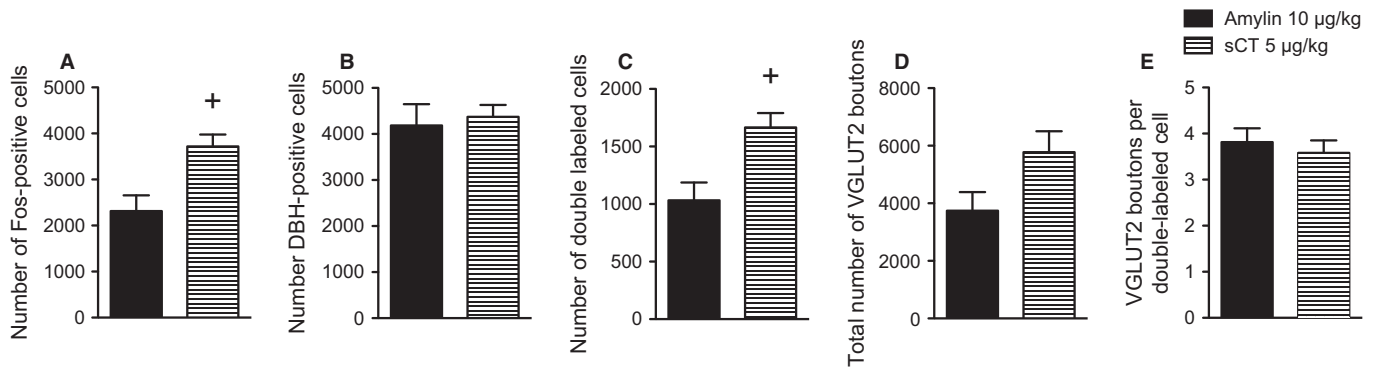

FIG. 6. Using confocal microscopy, approximately 50% of Fos-positive cells were also dopamine beta hydroxylase (DBH)-positive after amylin (10 μg/kg) and salmon calcitonin (sCT; 5 μg/kg), and there was a similar apposition of vesicular glutamate transporter-2 (VGLUT2)-positive boutons in amylin- (10 μg/kg) and sCT- (5 μg/kg) treated sham rats. Mean ± SEM unbiased estimation of the number of Fos-positive cells (A), DBH-positive cells (B), and Fos and DBH double-labeled cells (C) in the entire AP of sham rats treated with 10 μg/kg amylin or 5 μg/kg sCT, as quantified using confocal microscopy. Mean ± SEM unbiased estimation of the total number of VGLUT2-positive boutons apposed to neurons co-expressing Fos and DBH (D), and the average number of VGLUT2-positive boutons per double-labeled cell (E) in the entire AP of sham rats treated with 10 μg/kg amylin or 5 μg/kg sCT. +Significantly different from amylin (10 μg/kg) $P \leq 0.05$.

sCT treatment ($t_4 = 0.131$, $P = 0.9021$), as depicted in Fig. 7A. However, the light microscopy method appeared to underestimate the portion of DBH cells that co-express Fos, compared with confocal microscopy, in both amylin- ($t_5 = 3.496$, $P = 0.0174$) and sCT-treated groups ($t_4 = 5.703$, $P = 0.0047$; Fig. 7B).

Discussion

The AP is a critical brain area for the control of homeostatic nutrient handling. The AP relays information relating to gastric emptying, mediates the formation of conditioned taste aversion, and expresses receptors for many metabolic hormones including amylin, glucagon-like peptide-1 (GLP-1) and ghrelin (Edwards *et al.*, 1998; Fry & Ferguson, 2009; Punjabi *et al.*, 2011; Zuger *et al.*, 2013). The purpose of the present study was threefold. First, we characterized meal patterns in sham- and AP-lesioned rats under *ad libitum* and post-deprivation conditions. Second, we sought to clarify the role of the AP in sCT-induced anorexia over a range of doses, relative to the effect of amylin. Finally, we examined and compared the phenotype of brainstem neurons expressing amylin- and sCT-induced Fos, and thereby used for the first time the confocal microscopy approach to quantify cells in the AP.

Over the course of our experiments, and consistent with previous work done in our laboratory, it became evident that when using APX rats for behavioral experiments, which involved 12-h fasting, rats did not react the same way as their sham controls. APX rats had a long latency to eat and some did not start eating for up to 4 h into the dark phase. Earlier work with AP-lesioned rodents suggested that the AP plays a crucial role in the detection of inhibitory signals triggered by food or fluid ingestion, and that ingestive bouts increase in size after APX because the inhibitory feedback is blunted (Stricker *et al.*, 1997). It has also been proposed that because total daily food intake is similar in control and APX rats, APX disrupts the short-term control of meal pattern but not the long-term control of caloric intake in association with body weight maintenance (Ritter & Edwards, 1984). Consistent with these findings, our analysis of meal patterns showed that although APX and sham rats consumed comparable amounts of chow per day under *ad libitum* conditions, there were differences in how their meals were structured and how the two groups responded to a 12-h light phase fast. Under *ad libitum* conditions, APX ate larger but fewer meals compared with sham rats. Further, we observed that APX rats ingested a larger first meal after dark-onset than sham rats, but the latency to do so was much longer. After fasting the rats for 12 h during the light phase, sham rats compensated by eating more food over the subsequent 24-h period than under *ad libitum* conditions. They did so by increasing their average meal size and reducing the latency to feed after the fast. In contrast, the meal profile in APX rats remained almost unal-

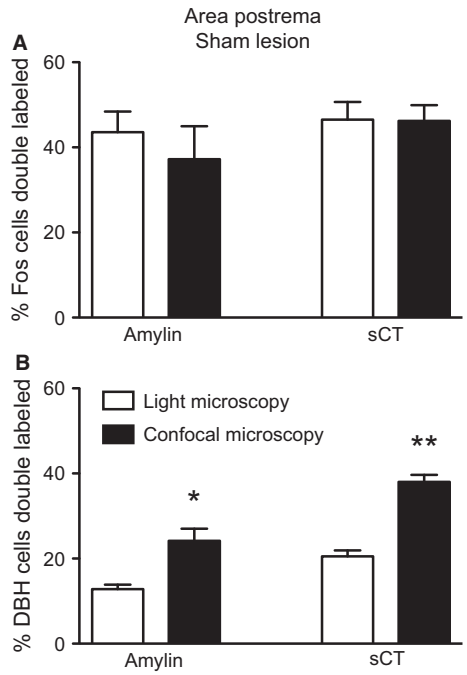

FIG. 7. Compared with confocal microscopy, light microscopy underestimated the degree of dopamine beta hydroxylase (DBH)-expressing neurons that also express Fos, but not Fos-expressing neurons that also express DBH. Mean ± SEM percentage of total Fos-positive cells that co-localize with DBH (A) and the percentage of total DBH-positive cells that co-localize with Fos (B) in the area postrema (AP) of sham rats treated with 10 μg/kg amylin or 5 μg/kg salmon calcitonin (sCT), as calculated using light microscopy and confocal microscopy methods of analysis. *Significantly different from light microscopy $P \leq 0.05$, **$P \leq 0.01$.

tered by the metabolic challenge; APX rats consumed even fewer meals than under *ad libitum* conditions and ate less over the subsequent 24 h. Hence, APX rats appeared unaffected by the preceding caloric deficit.

It was initially suggested that the disruption in ingestive patterns following AP lesions was a result of the loss of signals of gastric distention (Stricker *et al.*, 1997). Today we know that ablation of the AP not only thwarts a major relay station for vagal and splanchnic sensory information passing from the viscera to the brain, but also destroys several neuronal populations responsive to various hormones controlling food intake. Ablation of AP neurons prevents amylin-induced satiation thus increasing meal size (Lutz *et al.*, 1998; Reidelberger *et al.*, 2002; Potes *et al.*, 2010b). The loss of AP neurons carrying GLP-1 receptors (Yamamoto *et al.*, 2003), which likely constitute a neuronal population discrete from amylin-responsive neurons (Zuger *et al.*, 2013), is another potential contributor to the large extended meals observed following APX. The loss of a third receptor population could explain the increased latency to feed under both *ad libitum* and post-deprivation conditions. Ghrelin receptors are also present in the AP (Zigman *et al.*, 2006), and APX was previously shown to blunt ghrelin's orexigenic effect in rats at least under certain conditions (Gilg & Lutz, 2006). Further, ghrelin exerts a direct effect on the electrical activity of a subpopulation of AP neurons (Fry & Ferguson, 2009). Ghrelin signaling in the AP might be critical for both normal meal initiation and for enhancing food seeking and consumption after a fast. We suggest that the lack of ghrelin signaling might lead to the delayed initiation to feed in APX rats. A schematic of these AP neuronal populations is presented in Fig. 8.

In addition to the effects on hormone sensing, lesioning the AP also disrupts perception of various nutrients that can modify food intake. Not only have glucose-responsive neurons in the AP been identified (Adachi *et al.*, 1995), but the majority of amylin-sensitive

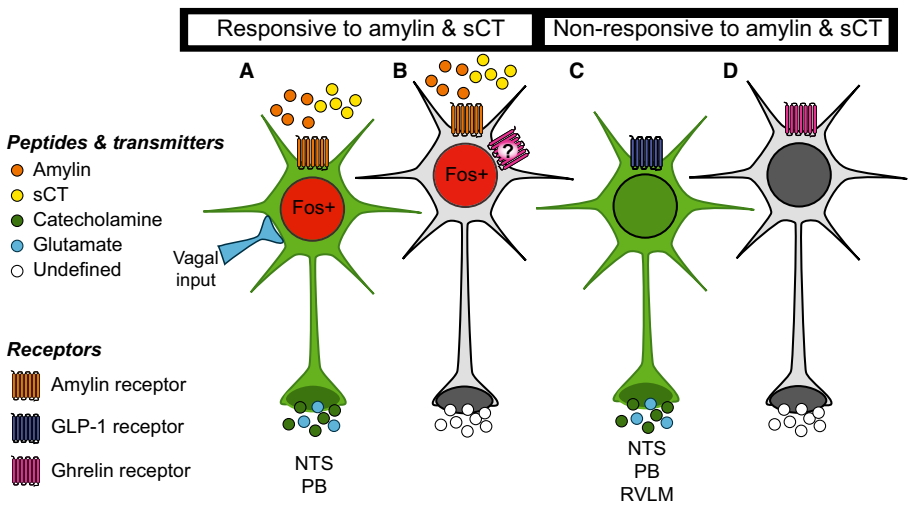

FIG. 8. Evidence-based schematic of phenotypes of neuronal populations in the area postrema (AP). Amylin- and salmon calcitonin (sCT)-activated neurons, as shown by Fos expression (red nucleus), can be dopamine beta hydroxylase (DBH)-positive (approximately 50%; green neurons in A) or unidentified (gray neurons in B), but do not express tryptophan hydroxylase (TPH). Some of the unidentified neurons could also be second-order neurons. Of the DBH neurons activated by amylin or sCT (A), 95% are apposed to vesicular glutamate transporter-2 (VGLUT2) boutons (cyan terminals), suggesting a glutamatergic input, possibly of vagal origin (Kalia & Sullivan, 1982). The amylin-activated neurons project to the nucleus of the solitary tract (NTS) and parabrachial nucleus (PB), where they hypothetically secrete catecholamines and glutamate (Stornetta *et al.*, 2002; Potes *et al.*, 2010a,b); these neurons can also respond to glucose (not shown; Riediger *et al.*, 2002). A third population of neurons express glucagon-like peptide-1 (GLP-1) receptors (blue) and are also DBH-positive (green neurons in C; Yamamoto *et al.*, 2003), but are likely distinct from the amylin-activated, catecholaminergic neurons because GLP-1-activated neurons do not express calcitonin receptor (CTR; Zuger *et al.*, 2013). These neurons project to the NTS, PB and ventrolateral medulla (RVLM) where they secrete catecholamines and glutamate (Stornetta *et al.*, 2002; Yamamoto *et al.*, 2003). Finally, a population of neurons responsive to ghrelin has also been identified (D; Fry & Ferguson, 2009). The phenotype of these neurons is not known; however, the ghrelin receptor (pink) does not co-localize to catecholaminergic neurons in the AP (Zigman *et al.*, 2006). At present, it is unknown if unidentified neurons activated by amylin and sCT (B) also bear ghrelin receptors.

neurons in the AP are also activated by glucose (Riediger *et al.*, 2002). Further, elegant new studies show that fasting-induced reduction of blood glucose actually promotes diffusion of blood-borne metabolic substrates, such as glucose, into the brain through changes in blood vessel fenestration and reorganization of tight junction complexes in the median eminence (Langlet *et al.*, 2013a). The AP is structurally similar to the median eminence, displaying a network of tanycyte-like cells and fenestrated capillaries (Langlet *et al.*, 2013b), and could potentially display similar plasticity during a metabolic challenge like fasting (Prevot *et al.*, 2013). If substrate receptivity of the AP does indeed depend on nutritional status, ablation of AP neurons would have clear ramifications on an organism's ability to sense and respond to a metabolic deficit, as we have shown herein. Finally, it was also recently shown that certain individual amino acids are capable of reducing food intake, but require an intact AP (Jordi *et al.*, 2013). The inability to sense these collective signals following APX likely contributes to the disruption of both spontaneous eating and the adaptive response to fasting.

In the second part of our studies, we found that, similar to amylin, an intact AP was necessary to produce the full anorectic action of sCT, confirming previous findings (Lutz *et al.*, 2001). Results from the dose–response study showed that at higher doses, sCT is capable of reducing food intake to a certain extent in APX rats. Thus, while sCT acting on the AP appears to be the primary route of action, we cannot rule out the possibility that sCT may also reduce food intake though an AP-independent mechanism or that a few remaining intact AP neurons are sufficient to mediate some reduction in eating after higher doses of sCT. A recent study suggests that the ventral tegmental area (VTA), a key brain center for reward processing, not only expresses all components of the amylin receptor, but also seems to play a role in the direct mediation of the effects of peripheral sCT on food intake (Mietlicki-Baase *et al.*, 2013); it was observed that local VTA administration of an amylin antagonist increased food intake and partly prevented the eating inhibitory effect of peripheral sCT. Therefore, in parallel to the immunohistochemical studies described here, we also analysed an additional series of tissue sections for the co-localization of the enzyme catalysing dopamine synthesis, tyrosine hydroxylase (TH) and Fos activation in AP- and sham-lesioned rats treated with either 10 μg/kg of amylin, 5 μg/kg of sCT or vehicle. Although TH-positive neurons were abundant in the VTA of all groups, no Fos was detected under our conditions (unpublished data). These data suggest that further investigation is required to determine the role of the VTA following peripheral treatment with amylin or sCT.

Despite the use of equipotent eating-inhibitory doses, sCT treatment produced a significantly higher number of Fos-positive neurons in the AP than amylin when analysed with either light or confocal analysis. This difference was likely the result of the ability of sCT to bind irreversibly and with higher affinity to amylin-binding sites. Given the high affinity of sCT, but not amylin, for the CTR subunit in the absence of RAMPs (Christopoulos *et al.*, 1999), theoretically, sCT could activate additional AP neurons expressing only the CTR subunit. However, emerging data from our lab show that 100% of single cells collected from the AP that express CTR also express RAMP1, RAMP3 or both subunits, suggesting that such a CTR-only population is not present in the AP (Liberini *et al.*, 2013). Despite increased activation in the AP, no difference in Fos was observed between sCT and amylin at the level of the NTS, and APX blocked all NTS Fos activation by both amylin and sCT. These results demonstrate that the NTS is a downstream relay of the AP neurons that mediates amylin and sCT eating-inhibitory activity. The neurotransmitters involved in this relay remain to be determined, however. The vast majority of AP neurons immunoreactive for TH also express VGLUT2 mRNA (Stornetta *et al.*, 2002), suggesting that these catecholaminergic neurons are indeed glutamatergic as well. Thus, it is possible that induction of Fos in the NTS is dependent upon glutamatergic input from AP neurons carrying the amylin receptor, but this has not been tested directly.

In addition to comparing Fos activation after amylin and sCT treatment, we also investigated if sCT recruited phenotypically different AP or NTS neurons than amylin. Confirming previously published results from our group, we found that approximately 50% of amylin-activated neurons in the AP are noradrenergic (Potes *et al.*, 2010b). Consistent with increased Fos expression, a slightly larger total number of sCT-induced Fos neurons co-expressed DBH, compared with amylin. Further, it has been suggested previously that an intact serotonergic system is necessary for calcitonin-induced analgesia (Ormazabal *et al.*, 2001). Because sCT also activates CTRs, we therefore sought to determine if this system plays a role in other actions, like the suppression of food intake. However, we observed almost no overlap between the expression of Fos and TPH in the AP, NTS, DR or CR. These findings support earlier results suggesting that the serotonergic system does not seem to mediate amylin-induced satiation (Lutz *et al.*, 1996; Brunetti *et al.*, 2002), and further demonstrate that activation of these serotonergic neurons is not necessary for sCT to suppress eating.

In the last part of our study, we employed confocal microscopy and stereology to refine our study of neuronal activation patterns of the entire AP. First, we determined the apposition of VGLUT2-positive boutons to amylin- and sCT-activated neurons. While not specifically identified in this study, glutamatergic input to the AP likely arises primarily from vagal afferents (Kalia & Sullivan, 1982), and possibly also from the NTS (Potes *et al.*, 2010a). A difference in the number of VGLUT2 boutons per activated neuron, which may suggest a difference in the excitatory drive to this population of AP neurons, could potentially contribute to the stronger and in particular the longer inhibition of feeding observed after sCT, compared with amylin. However, we found that almost all (approximately 95%) amylin- and sCT-activated neurons were in contact with VGLUT2 boutons, and we did not observe a difference between amylin and sCT in the number of VGLUT2 appositions per double-labeled neuron. These results suggest that, at least following acute treatment, there is no difference in glutamatergic apposition between neurons activated by amylin or sCT. We did not determine if chronic treatment of amylin or sCT would modify the glutamatergic drive of these populations. Finally, we used the confocal method to estimate the co-expression of amylin- and sCT-induced Fos and DBH labeling across the whole AP. To our knowledge, this is the first attempt to determine an absolute quantification of Fos-, DBH- and VGLUT2-positive neurons in the AP. This analysis validated our light microscopy method of analysis, confirming that about 50% of amylin- and sCT-induced Fos-positive neurons co-localize with DBH. The traditional light microscopy approach did, however, underestimate the number of DBH neurons co-expressing Fos, which likely results from the inability to clearly distinguish closely apposed DBH-positive neurons in the z-plane without confocal imaging.

The results from our current study underscore the role of the AP in controlling short-term food intake. The meal pattern analysis showed that a lesion of the AP disrupts the negative feedback signals controlling meal size and seems to affect the ability to compensate for an energy deficit following a fast. Further, we found that, like amylin, sCT requires an intact AP to produce its full effect on food intake and to induce Fos in the NTS. We observed that neither peptide induced Fos in TPH-expressing neurons in the NTS, DR or CR, and detected no difference in the number of

VGLUT2 boutons apposed to amylin- or sCT-activated neurons expressing DBH. Use of confocal microscopy confirmed that, like amylin, approximately 50% of sCT-activated neurons in the AP are noradrenergic. The phenotype of the remaining Fos-positive neurons in the AP remains to be defined. A summary of our findings, in relation to the existing literature, is depicted in Fig. 8. Our study demonstrates that amylin and its agonist sCT activate similar neuronal populations, suggesting that the difference in anorexic potency between the peptides primarily results from differences in binding affinity and receptor dissociation.

Acknowledgements

This work was supported by Novo Nordisk and the Swiss National Science Foundation, and LA was supported by NIH DK 092608. The authors gratefully acknowledge the technical guidance and assistance of Dr Lutz Slomianka, Dr Kathrin Abegg and Dr Urs Ziegler. Imaging was performed with support of the Center for Microscopy and Image Analysis, University of Zurich.

Abbreviations

AP, area postrema; APX, area postrema lesion/lesioned; CR, central raphe nucleus; CTR, calcitonin receptor; DAB, 3,3′-diaminobenzidene-tetrahydrochloride; DBH, dopamine beta hydroxylase; DR, dorsal raphe nucleus; GLP-1, glucagon-like peptide-1; i.p., intraperitoneal; NDS, normal donkey serum; NGS, normal goat serum; NTS, nucleus of the solitary tract; NTSm, medial subnucleus of the nucleus of the solitary tract; PB, phosphate buffer; RAMP, receptor activity-modifying protein; sCT, salmon calcitonin; TH, tyrosine hydroxylase; TPH, tryptophan hydroxylase; VGLUT2, vesicular glutamate transporter-2; VTA, ventral tegmental area.

References

Adachi, A., Kobashi, M. & Funahashi, M. (1995) Glucose-responsive neurons in the brainstem. *Obes. Res.*, **3**(Suppl. 5), 735S–740S.

Barth, S.W., Riediger, T., Lutz, T.A. & Rechkemmer, G. (2004) Peripheral amylin activates circumventricular organs expressing calcitonin receptor a/b subtypes and receptor-activity modifying proteins in the rat. *Brain Res.*, **997**, 97–102.

Boyle, C.N., Lorenzen, S.M., Compton, D. & Watts, A.G. (2012) Dehydration-anorexia derives from a reduction in meal size, but not meal number. *Physiol. Behav.*, **105**, 305–314.

Brunetti, L., Recinella, L., Orlando, G., Michelotto, B., Di Nisio, C. & Vacca, M. (2002) Effects of ghrelin and amylin on dopamine, norepinephrine and serotonin release in the hypothalamus. *Eur. J. Pharmacol.*, **454**, 189–192.

Butler, P.C., Chou, J., Carter, W.B., Wang, Y.N., Bu, B.H., Chang, D., Chang, J.K. & Rizza, R.A. (1990) Effects of meal ingestion on plasma amylin concentration in NIDDM and nondiabetic humans. *Diabetes*, **39**, 752–756.

Christopoulos, G., Perry, K.J., Morfis, M., Tilakaratne, N., Gao, Y., Fraser, N.J., Main, M.J., Foord, S.M. & Sexton, P.M. (1999) Multiple amylin receptors arise from receptor activity-modifying protein interaction with the calcitonin receptor gene product. *Mol. Pharmacol.*, **56**, 235–242.

Edwards, G.L., Gedulin, B.R., Jodka, C., Dilts, R.P., Miller, C.C. & Young, A. (1998) Area postrem (AP)-lesions block the regulation of gastric emptying by amylin. *Neurogastroent. Motil.*, **10**, 26.

Fry, M. & Ferguson, A.V. (2009) Ghrelin modulates electrical activity of area postrema neurons. *Am. J. Physiol.-Reg. I.*, **296**, R485–R492.

Fukuda, T., Hirai, Y., Maezawa, H., Kitagawa, Y. & Funahashi, M. (2013) Electrophysiologically identified presynaptic mechanisms underlying amylinergic modulation of area postrema neuronal excitability in rat brain slices. *Brain Res.*, **1494**, 9–16.

Gilg, S. & Lutz, T.A. (2006) The orexigenic effect of peripheral ghrelin differs between rats of different age and with different baseline food intake, and it may in part be mediated by the area postrema. *Physiol. Behav.*, **87**, 353–359.

Gundersen, H.J., Jensen, E.B., Kieu, K. & Nielsen, J. (1999) The efficiency of systematic sampling in stereology–reconsidered. *J. Microsc.*, **193**, 199–211.

Jordi, J., Herzog, B., Camargo, S.M., Boyle, C.N., Lutz, T.A. & Verrey, F. (2013) Specific amino acids inhibit food intake via the area postrema or vagal afferents. *J. Physiol.*, **591**, 5611–5621.

Kalia, M. & Sullivan, J.M. (1982) Brainstem projections of sensory and motor components of the vagus nerve in the rat. *J. Comp. Neurol.*, **211**, 248–265.

Langlet, F., Levin, B.E., Luquet, S., Mazzone, M., Messina, A., Dunn-Meynell, A.A., Balland, E., Lacombe, A., Mazur, D., Carmeliet, P., Bouret, S.G., Prevot, V. & Dehouck, B. (2013a) Tanycytic VEGF-A boosts blood-hypothalamus barrier plasticity and access of metabolic signals to the arcuate nucleus in response to fasting. *Cell Metab.*, **17**, 607–617.

Langlet, F., Mullier, A., Bouret, S.G., Prevot, V. & Dehouck, B. (2013b) Tanycyte-like cells form a blood-cerebrospinal fluid barrier in the circumventricular organs of the mouse brain. *J. Comp. Neurol.*, **521**, 3389–3405.

Liberini, C., Boyle, C.N. & Lutz, T.A. (2013) Gene expression profiling of single amylin-activated neuron in the rat area postrema *2013 Neuroscience Meeting Planner*. Society for Neuroscience, [Internet] San Diego, CA.

Lutz, T.A. (2012) Control of energy homeostasis by amylin. *Cell. Mol. Life Sci.*, **69**, 1947–1965.

Lutz, T.A., Del Prete, E., Walzer, B. & Scharrer, E. (1996) The histaminergic, but not the serotoninergic, system mediates amylin's anorectic effect. *Peptides*, **17**, 1317–1322.

Lutz, T.A., Senn, M., Althaus, J., Del Prete, E., Ehrensperger, F. & Scharrer, E. (1998) Lesion of the area postrema/nucleus of the solitary tract (AP/NTS) attenuates the anorectic effects of amylin and calcitonin gene-related peptide (CGRP) in rats. *Peptides*, **19**, 309–317.

Lutz, T.A., Tschudy, S., Rushing, P.A. & Scharrer, E. (2000) Amylin receptors mediate the anorectic action of salmon calcitonin (sCT). *Peptides*, **21**, 233–238.

Lutz, T.A., Mollet, A., Rushing, P.A., Riediger, T. & Scharrer, E. (2001) The anorectic effect of a chronic peripheral infusion of amylin is abolished in area postrema/nucleus of the solitary tract (AP/NTS) lesioned rats. *Int. J. Obes. Relat. Metab. Disord.*, **25**, 1005–1011.

Mack, C.M., Soares, C.J., Wilson, J.K., Athanacio, J.R., Turek, V.F., Trevaskis, J.L., Roth, J.D., Smith, P.A., Gedulin, B., Jodka, C.M., Roland, B.L., Adams, S.H., Lwin, A., Herich, J., Laugero, K.D., Vu, C., Pittner, R., Paterniti, J.R. Jr., Hanley, M., Ghosh, S. & Parkes, D.G. (2010) Davalintide (AC2307), a novel amylin-mimetic peptide: enhanced pharmacological properties over native amylin to reduce food intake and body weight. *Int. J. Obesity*, **34**, 385–395.

Mietlicki-Baase, E.G., Rupprecht, L.E., Olivos, D.R., Zimmer, D.J., Alter, M.D., Pierce, R.C., Schmidt, H.D. & Hayes, M.R. (2013) Amylin receptor signaling in the ventral tegmental area is physiologically relevant for the control of food intake. *Neuropsychopharmacology*, **38**, 1685–1697.

Muff, R., Buhlmann, N., Fischer, J.A. & Born, W. (1999) An amylin receptor is revealed following co-transfection of a calcitonin receptor with receptor activity modifying proteins-1 or -3. *Endocrinology*, **140**, 2924–2927.

Ogawa, A., Harris, V., McCorkle, S.K., Unger, R.H. & Luskey, K.L. (1990) Amylin secretion from the rat pancreas and its selective loss after streptozotocin treatment. *J. Clin. Invest.*, **85**, 973–976.

Ormazabal, M.J., Goicoechea, C., Sanchez, E. & Martin, M.I. (2001) Salmon calcitonin potentiates the analgesia induced by antidepressants. *Pharmacol. Biochem. Be.*, **68**, 125–133.

Potes, C.S., Lutz, T.A. & Riediger, T. (2010a) Identification of central projections from amylin-activated neurons to the lateral hypothalamus. *Brain Res.*, **1334**, 31–44.

Potes, C.S., Turek, V.F., Cole, R.L., Vu, C., Roland, B.L., Roth, J.D., Riediger, T. & Lutz, T.A. (2010b) Noradrenergic neurons of the area postrema mediate amylin's hypophagic action. *Am. J. Physiol.-Reg. I.*, **299**, R623–R631.

Prevot, V., Langlet, F. & Dehouck, B. (2013) Flipping the tanycyte switch: how circulating signals gain direct access to the metabolic brain. *Aging*, **5**, 332–334.

Punjabi, M., Arnold, M., Geary, N., Langhans, W. & Pacheco-Lopez, G. (2011) Peripheral glucagon-like peptide-1 (GLP-1) and satiation. *Physiol. Behav.*, **105**, 71–76.

Reidelberger, R.D., Kelsey, L. & Heimann, D. (2002) Effects of amylin-related peptides on food intake, meal patterns, and gastric emptying in rats. *Am. J. Physiol.-Reg. I.*, **282**, R1395–R1404.

Riediger, T., Schmid, H.A., Young, A.A. & Simon, E. (1999) Pharmacological characterisation of amylin-related peptides activating subfornical organ neurones. *Brain Res.*, **837**, 161–168.

Riediger, T., Schmid, H.A., Lutz, T.A. & Simon, E. (2002) Amylin and glucose co-activate area postrema neurons of the rat. *Neurosci. Lett.*, **328**, 121–124.

Riediger, T., Zuend, D., Becskei, C. & Lutz, T.A. (2004) The anorectic hormone amylin contributes to feeding-related changes of neuronal activity in key structures of the gut-brain axis. *Am. J. Physiol.-Reg. I.*, **286**, R114–R122.

Ritter, R.C. & Edwards, G.L. (1984) Area postrema lesions cause overconsumption of palatable foods but not calories. *Physiol. Behav.*, **32**, 923–927.

Rowland, N.E. & Richmond, R.M. (1999) Area postrema and the anorectic actions of dexfenfluramine and amylin. *Brain Res.*, **820**, 86–91.

Rowland, N.E., Crews, E.C. & Gentry, R.M. (1997) Comparison of Fos induced in rat brain by GLP-1 and amylin. *Regul. Peptides*, **71**, 171–174.

Sexton, P.M., Paxinos, G., Kenney, M.A., Wookey, P.J. & Beaumont, K. (1994) *In vitro* autoradiographic localization of amylin binding sites in rat brain. *Neuroscience*, **62**, 553–567.

Stornetta, R.L., Sevigny, C.P. & Guyenet, P.G. (2002) Vesicular glutamate transporter DNPI/VGLUT2 mRNA is present in C1 and several other groups of brainstem catecholaminergic neurons. *J. Comp. Neurol.*, **444**, 191–206.

Stricker, E.M., Curtis, K.S., Peacock, K.A. & Smith, J.C. (1997) Rats with area postrema lesions have lengthy eating and drinking bouts when fed *ad libitum*: implications for feedback inhibition of ingestive behavior. *Behav. Neurosci.*, **111**, 623–632.

West, M.J., Slomianka, L. & Gundersen, H.J. (1991) Unbiased stereological estimation of the total number of neurons in thesubdivisions of the rat hippocampus using the optical fractionator. *Anat. Rec.*, **231**, 482–497.

Wimalawansa, S.J. (1997) Amylin, calcitonin gene-related peptide, calcitonin, and adrenomedullin: a peptide superfamily. *Crit. Rev. Neurobiol.*, **11**, 167–239.

Yamamoto, H., Kishi, T., Lee, C.E., Choi, B.J., Fang, H., Hollenberg, A.N., Drucker, D.J. & Elmquist, J.K. (2003) Glucagon-like peptide-1-responsive catecholamine neurons in the area postrema link peripheral glucagon-like peptide-1 with central autonomic control sites. *J. Neurosci.*, **23**, 2939–2946.

Zigman, J.M., Jones, J.E., Lee, C.E., Saper, C.B. & Elmquist, J.K. (2006) Expression of ghrelin receptor mRNA in the rat and the mouse brain. *J. Comp. Neurol.*, **494**, 528–548.

Zuger, D., Forster, K., Lutz, T.A. & Riediger, T. (2013) Amylin and GLP-1 target different populations of area postrema neurons that are both modulated by nutrient stimuli. *Physiol. Behav.*, **112–113**, 61–69.